ChemComm

COMMUNICATION

View Article Online
View Journal

Cite this: DOI: 10.1039/c6cc00303f

Received 12th January 2016,
Accepted 14th March 2016

DOI: 10.1039/c6cc00303f

www.rsc.org/chemcomm

Nanowire growth kinetics in aberration corrected environmental transmission electron microscopy†

Yi-Chia Chou,*[abc] Federico Panciera,[cd] Mark C. Reuter,[c] Eric A. Stach[a] and Frances M. Ross*[c]

We visualize atomic level dynamics during Si nanowire growth using aberration corrected environmental transmission electron microscopy, and compare with lower pressure results from ultra-high vacuum microscopy. We discuss the importance of higher pressure observations for understanding growth mechanisms and describe protocols to minimize effects of the higher pressure background gas.

Semiconductor nanostructures present exciting possibilities for electronic and energy applications. In particular, catalytic growth of Si, Ge and III–V materials by the vapor–liquid–solid (VLS) or vapor–solid–solid (VSS) mechanisms can produce nanowires with morphology, dimensions, and electronic properties that are potentially suitable for deep scaling of electronic devices, as well as applications in sensors, batteries and photovoltaics. From both a scientific and technological perspective, precise control of the final structure formed by the VSS and VLS processes requires an understanding of the atomic-level details of growth.

In VLS and VSS growth, the source material is supplied from a precursor gas, dissolves into nanoscale catalysts and precipitates at the catalyst/substrate interface. The catalyst is liquid or solid for VLS and VSS growth, respectively. For Si and Ge, both VLS and VSS processes have been examined using *in situ* electron microscopy;[1–13] a full list of citations is given in ref. 1. *In situ* observations show, for example, the VLS process by which liquid eutectic droplets of AuSi form when Au is deposited on Si, and their subsequent catalytic action in forming Si nanowires.[1–5] Si with Al[6] and Ge with Au[7] are other examples of VLS systems. VSS growth has been imaged *in situ* using other catalytic metals: Cu[8] and Pd[9] form solid silicides that catalyze Si nanowire growth, while AuAg[10] or AuAl[11] alloys can form either solid or liquid catalysts, depending on temperature and alloy composition. The *in situ* experiments show that in all cases Si grows by repeated nucleation and flow of 0.3 nm height (atomic bilayer) steps at the catalyst/nanowire interface;[1,9] growth models derived from *in situ* observations explain step flow kinetics and interface morphology[12,13] and the effect of catalyst phase on compositional profiles,[10,11] helpful in designing device structures.

The majority of these *in situ* observations have been made under ultra-high vacuum (UHV) conditions.[1–4,6–8,10–13] UHV microscopy (UHV-TEM) offers clean surfaces and well-controlled growth kinetics due to the low background pressure, $\sim 10^{-10}$ Torr.[1] However, vacuum design also restricts the pressure during growth to below $\sim 10^{-5}$ Torr. In conventional reactors, Si and Ge (and III–V) nanowires are grown at higher pressures and not under UHV conditions.[14,15] This means that there is a "pressure gap" between the conditions used for microscopy observation and the conditions for real-life growth. Such a pressure gap is familiar in catalysis studies[16] and has been narrowed, if not completely closed, through the use of environmental TEM (ETEM).[17] ETEM offers a higher pressure during imaging, up to several Torr, but with a base pressure, $\sim 10^{-6}$ Torr, that is not as low as for UHV-TEM. Some ETEMs also provide the capability of aberration-corrected imaging, with the exciting prospect of growth information with higher spatial resolution[18] than available from either conventional ETEM or UHV-TEM. Furthermore, several modern detector designs[19] can provide temporal resolution of several hundred images per second, an improvement over the 30 fps typically obtained in UHV-TEM or conventional ETEM, and also allowing opportunities such as dose fractionation, which can reduce the effect of sample drift.

Here we describe a direct view of the dynamic processes taking place at the interfaces between nanowires and their catalysts, at the pressures available in ETEM, and with aberration-corrected spatial resolution and high temporal resolution. We grow Si nanowires from liquid AuSi, liquid AuAgSi and solid AuAg catalysts and image the morphology at the growth interface, the catalyst structure, the step height and step flow kinetics. We find that aberration-corrected imaging with high image acquisition rates provides useful structural

---

[a] *Center for Functional Nanomaterials, Brookhaven National Laboratory, Upton, NY, USA*
[b] *Department of Electrophysics, College of Science, National Chiao Tung University, Hsinchu, Taiwan. E-mail: ycchou@nctu.edu.tw*
[c] *IBM T. J. Watson Research Center, Yorktown Heights, NY, USA. E-mail: fmross@us.ibm.com*
[d] *Engineering Department, University of Cambridge, Cambridge, UK*

† Electronic supplementary information (ESI) available: Details of experimental procedure; surface layer formation in ETEM; effect of surface layer on kinetics; movie captions; Movies M1–M5. See DOI: 10.1039/c6cc00303f

information for both solid and liquid catalysts. However, quantitative comparison between the information obtained in ETEM and in UHV-TEM shows distinct differences in kinetics. We show that the higher gas pressures in ETEM coupled with the greater intensity of beam at the sample modify the catalyst and nanowire surface and alter the growth kinetics. We describe protocols to mitigate the effects of the non-UHV, higher pressure environment. This allows growth to be probed over a higher range of pressures and with atomic resolution to contribute to a mechanistic understanding of nanowire growth. We discuss growth kinetics, corner facets and liquid ordering. Finally, since Si nanowire growth is one of the few systems where ETEM experiments can be compared with those obtained under UHV conditions, we discuss the relevance of these results to interpretation of ETEM data obtained during other dynamic processes.

A Si nanowire imaged during VLS growth using aberration-corrected ETEM is shown in Fig. 1a and Movie 1a (ESI†). The growth rate is 3.8 nm s^{-1} (Fig. 1c) in this example. UHV-TEM experiments can only probe slower growth (rates achievable are <1 nm s^{-1} at 10^{-5} Torr and similar T), so this shows the usefulness of the higher pressure in accessing a greater range of kinetics. Overall, nanowires growing in ETEM appear similar to those grown in UHV-TEM – for example, the flat Si(111) growth interface is visible – but additional information is provided by the higher resolution. The narrow dark contrast visible at the nanowire sidewalls is consistent with a surface layer of Au.[20] Au surface decoration during growth was implied indirectly from *ex situ* observations.[1,21] Growth proceeds by rapid flow of steps at the growth interface (Movie 1a, ESI†). In this particular experiment, each step flows quickly enough that a layer is completed within the time resolution of the movie; there is then a ~0.05 s pause before the next step flows. Such pause-flow kinetics are expected from models that include the droplet chemical energy and barrier for step nucleation.[7,8] The temporal and spatial resolution of the image series allows us to provide a lower limit of ~1–2 μm s^{-1} on the step flow speed.

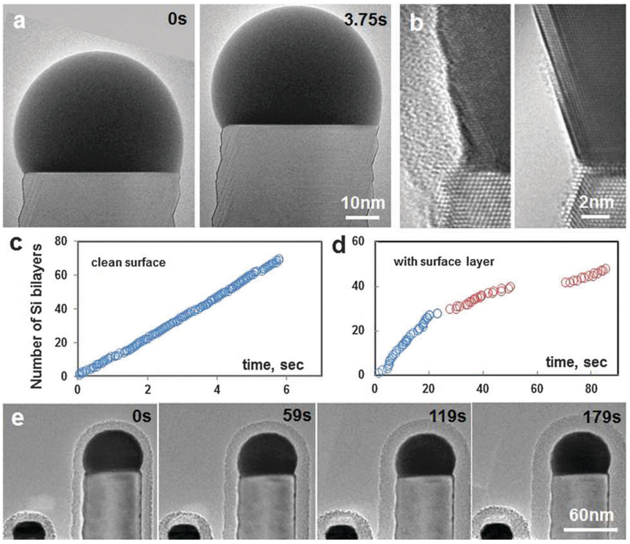

Fig. 1 Si nanowire growth recorded using ETEM at 400 images per second. (a) VLS growth of a Si nanowire from AuSi at 500 °C and 2 × 10^{-5} Torr disilane. Note the clean appearance of the surfaces. (b) Si nanowire formed by VSS from AuAg in the UHVTEM, then transferred to the ETEM and imaged at RT. A surface oxide formed by the air exposure (left image) was removed (right) by focusing the beam on the nanowire without raising T, revealing a faceted catalyst surface. (c) Growth rate for the nanowire in (a) with clean surface. (d) Growth rate for the nanowire in Fig. S1, ESI† (AuAgSi liquid catalyst, 425 °C, 5 × 10^{-3} Torr disilane), with amorphous surface layer. (e) Si nanowire formed by VLS from Au in the UHVTEM, then transferred to the ETEM and imaged at 550 °C in 6 × 10^{-3} Torr disilane. No growth occurs; instead an amorphous shell forms.

In order to obtain such data, it was important to control the growth environment using techniques that we describe below. The nanowire in Fig. 1a appears clean, but earlier experiments yielded images like that in Fig. 1b (left image) or Fig. S1 (ESI†), where amorphous surface layers are visible. We find that, unsurprisingly, such surface layers strongly affect growth kinetics, persisting at elevated temperature and slowing or suppressing VLS and VSS growth during ETEM observations. Presumably the layers are composed of oxides that formed in air on the catalyst surface and prevent the source gas from reaching the catalyst. An example of the growth kinetics measured under such circumstances is shown in Fig. 1d. Note the difference in scale compared to Fig. 1c; growth is ~20× slower. Also note the irregularity of growth in comparison to Fig. 1c and especially to the highly regular growth curves measured in UHV-TEM.[12] Surface layers are not fully removed with HF vapor (see ESI†). It is possible to remove the layer by sputtering using a focused electron beam, a well-known phenomenon[22] (Fig. 1b). Needless to say, such treatment alters the sample but does provide a clean surface to enable growth to start.

However, once growth does begin, we observe an additional surface layer formation (Fig. 1e and Movie 1b, ESI†). Energy loss spectroscopy shows that this layer is SiO_x and does not contain carbon (Fig. S2, ESI†). The formation of this layer requires irradiation (it does not form outside the beam) and the presence of disilane (either during growth, or as a low pressure background due to incomplete pump-down after a previous growth experiment; see below). High temperatures are not required, as we observe layer formation at room temperature (ESI†). Under UHV conditions[1] such amorphous surface layers do not form, even under prolonged irradiation at high temperatures in the presence of disilane. We therefore attribute the layer formation to chemical reactions between the electron beam and oxidizing background gases (*i.e.* water vapor or oxygen) in the ETEM, which is not a UHV system. This reaction mechanism follows the principles of environmental scanning electron microscopy[23] where water vapor is ionized by the electron beam to form highly reactive species that (in our case) crack the disilane to result in SiO_x. Oxygen may act in the same way. The 300 kV primary beam has a low inelastic cross section with water vapor but the secondary electrons emitted when the primary beam hits the sample have a higher cross section and may be the main cause of the reaction.[24] Once the shell forms, it slows or prevents Si from dissolving into the catalyst. Nanowire growth may be slowed or stopped, and growth does not proceed smoothly because the oxide shell pins the catalyst/nanowire interface and prevents it advancing.

Avoiding this beam effect, with its impact on nanowire growth, requires removal of water vapor or oxygen from the background to achieve UHV levels (10^{-10} Torr). But even without a UHV system we can mitigate the effects of water vapor or oxygen in ETEM. Water vapor is generally reduced in conventional TEM by condensing it using a cold finger cooled by liquid nitrogen (boiling point −195.8 °C/77.4 K). This method can not be used in growth experiments involving disilane since it would condense the disilane (boiling point −14 °C/259 K) along with the water. We used a mixture of dry ice (sublimates at −78.5 °C/194.7 K) and ethanol (melting point −114 °C/159 K, boiling point 78.4 °C/351.5 K) in order to set the temperature of the cold finger at the sublimation temperature of dry ice. At this temperature the water vapor is still efficiently condensed while a sufficient fraction of the introduced disilane remains in its gaseous state and cracks at the catalyst surface. We finally note that the surface layer can form without deliberately flowing disilane, if there is residual disilane from incomplete pumping after a previous growth experiment (Fig. S2, ESI†). Flowing O_2 to react with and remove residual disilane slowed layer formation. However, completely stopping layer formation required venting the microscope, which effectively removed the residual disilane. This step is dramatic but appears necessary for avoiding layer growth in subsequent experiments.

By using the above procedures it was possible to obtain clean nanowire growth not only with AuSi, as shown in Fig. 1a, but also with catalysts based on metal alloys. Alloy catalysts, such as AuAg and AuAl, can operate in both VLS and VSS modes, with growth by VSS at lower temperatures and VLS at higher temperatures.[10,11] This is because in the AuAg–Si or AuAl–Si pseudobinary systems the eutectic temperatures to be selected to obtain either mode.

VLS growth experiments are shown in Fig. S1c and Movie 2a (ESI†). VLS growth with metal alloy catalysts appears similar to AuSi, with a flat interface between Si and the liquid across which individual bilayer-height steps flow rapidly. During growth we frequently find junctions between facets at the growth interface, as in Fig. 2a. (Such geometry is especially frequent if the nanowire surface is not completely clean and pins the trijunction during growth.) Aberration correction allows the structure of the nanowire/liquid interface and the edge where facets meet to be resolved during growth, Fig. 2a and b. First note the lack of visible ordering in the liquid adjacent to the solid. Ordering at liquid interfaces has been observed in other materials systems[25] but is not evident in this liquid catalyst. Also present at the corner is a small truncated section that can be identified as a (200) facet. The dynamic behavior of this facet is shown in Movie 2b (ESI†). Its size fluctuates as layers are added and removed at the nanowire/catalyst interface. However, the corner remains faceted: we do not observe an atomically sharp configuration during the experiment. Previous observations of dynamic changes in small facets during Si nanowire growth in UHV-TEM lacked the resolution to determine whether the facet is present at all times. The presence or absence of a higher index facet at an edge where larger facets meet is commonly understood *via* the Wulff construction. However, the Wulff construction is based on an equilibrium crystal, and in principle does not apply during growth. Instead, it has been suggested that small facets should be sensitive to the supersaturation of Si in the liquid and should therefore grow and shrink with the nucleation of steps.[12] The observation in Fig. 2b is consistent with the model.

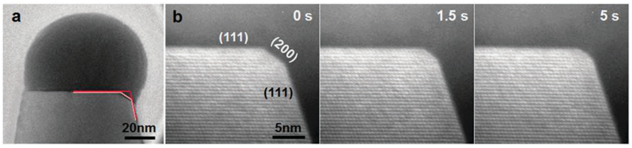

Fig. 2 Si nanowire growth by VLS from AuAgSi. (a) Overview of a nanowire with an enclosed facet during growth at 370 °C and 1.5 × 10^{-3} Torr disilane. (b) Bright field ETEM image sequence of the truncated corner in (a) during growth.

The importance of this observation lies in understanding nucleation energetics for Si growth. During growth, new layers are expected to nucleate at the periphery of the (111) growth plane. Creating a nucleus at the periphery also extends the facet that bounds the growth plane. Thus, the energy barrier for nucleation will depend on which facets bound the growth plane. Observations such as those in Movie 2 (ESI†) that can measure fluctuations in bounding facets may provide a basis for improved calculations of nucleation energetics.[26]

VSS growth is an important mode that is well-known in several materials systems;[14] the growth species is assumed to diffuse through the solid particle to the growth front. VSS growth with metal alloy catalysts in aberration corrected ETEM is shown in Fig. 3a and c for the example of Si growth from AuAg. For comparison, Fig. 3b and d shows growth under UHV conditions.

The orientation relation between Si and AuAg lattices and the overall truncated octahedron shape of the solid AuAg are consistent between ETEM and UHV TEM (Movie 3, ESI†).[10] Interface dynamics involve step flow in both cases but there are intriguing differences in step geometry. The steps in Fig. 3a and b are a single Si bilayer in height (0.3 nm) but those in Fig. 3c and d are triple height, composed of three Si bilayers (0.9 nm). We observe flow of single

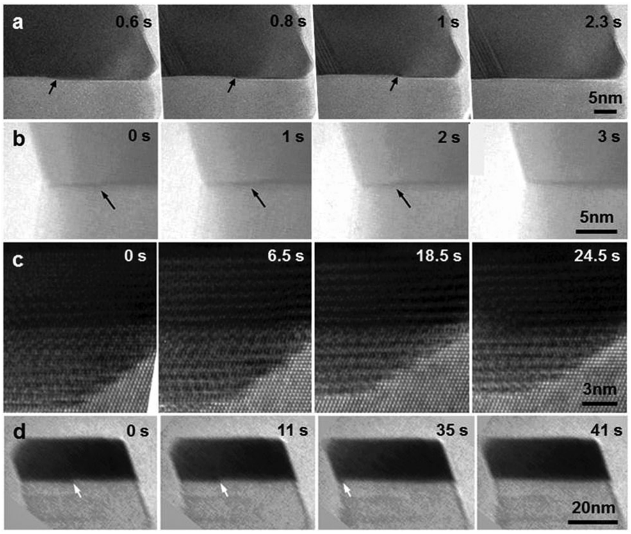

Fig. 3 Si nanowire growth, interface structure and step flow at solid AuAg/Si interfaces. (a) Image sequence showing a Si step with single Si bilayer moving along the interface with AuAg at 450 °C and 5 × 10^{-4} disilane in ETEM. (b) Image sequence showing a Si step (arrowed) with single Si bilayer moving along the interface with AuAg at 483 °C and 9.3 × 10^{-6} Torr disilane in UHV-TEM. (c) Image sequence showing dynamics at an inclined interface between solid AuAg and Si at 380 °C and 1.5 × 10^{-3} Torr disilane in ETEM. Rearrangement occurs by the motion of units of height 3 Si bilayers/4 AuAg layers. The longer period contrast in the AuAg is a moiré effect due to overlap with Si in projection. (d) Image sequence showing a Si step (arrowed) with triple Si bilayers moving along the interface with AuAg at 470 °C and 3 × 10^{-5} Torr disilane in UHV-TEM. The step flows in a [211] direction on the (111) plane. The contrast lower down is caused by twinning in the Si due to temperature changes during the experiment.

bilayer steps in ETEM if the surface is clean, but triple bilayer steps in the presence of the surface layer described above. Since the surface layer prohibited or slowed dissolution of Si into the catalyst, the process taking place could more accurately be described as interface rearrangement rather than growth of Si. In UHV-TEM, single height steps were common and triple height steps (Fig. 3d) were observed only for a small diameter nanowire that grew slowly even at higher pressure. We suggest that triple height steps may be preferred during, for example, rearrangement between solid catalyst and Si, because of the good lattice match between three Si bilayers and four AuAg planes (the mismatch between AuAg and Si is 24.9%).[10] The mismatch also leads to a periodic structure in-plane along the interface (Fig. S3a, ESI†) with one dislocation every 0.95 nm.

VSS growth is expected to show different kinetics compared to VLS since atomic level details of the solid/solid interface such as step height and local strain fields should influence the growth mechanism. Steps at the solid AuAg/Si interface move relatively slowly during growth, compared to the rapid VLS step motion in Fig. 1a. The slow VSS step dynamics has been explained through models[11,13] where the low solubility of Si in the solid catalyst makes it energetically favorable for Si to precipitate at the growth interface as soon as it arrives from the gas phase. Thus, Si adds gradually to an existing step, and nucleation of a new step takes place shortly after the previous layer has completed. These models do not include atomic level details of the interface, but such details are expected to affect step motion. We observe that steps do not flow smoothly. In Movie 3 (ESI†), motion is jerky and pinned at some points, similar to observations in other VSS systems[8,10,13] where pinning appears to be related to interfacial dislocations.

We finally note intriguing changes in the overall catalyst shape during VSS growth experiments. Fig. 4a and Movie 3d (ESI†) hint that during UHV growth, the catalyst shape changes periodically as steps flow during growth. A truncated corner fills during step flow then the facet size jumps as a new step starts. In ETEM, rearrangement of the solid catalyst surface is also visible (Fig. S3, S4 and Movie 4a, b, ESI,† Fig. 4b) but without the clear synchronization with interfacial step flow seen in UHV-TEM. We suggest that the nanoparticle as a whole may rearrange as steps flow to satisfy considerations of energy minimization.[27]

In conclusion, we have shown that aberration-corrected ETEM can reveal detailed features of step flow kinetics, facets at the nanowire/catalyst interface, and rearrangement of the solid catalyst surface. High resolution allows atomic configurations to be characterized, including individual events during the flow of steps. However, surface layers form in ETEM and the kinetics for Si incorporation differ compared to observations made during growth under UHV conditions. In ETEM, we suggest that surface layers form through reaction of the electron beam with residual oxygen or water vapor in the microscope vacuum. It is therefore essential to include beam effects when interpretating growth kinetics obtained in a non-UHV system. The detailed knowledge that already exists for nanowire growth under UHV is useful in disentangling beam effects and side reactions. But in other materials systems, where conclusions on reaction mechanisms are based on ETEM, we need to consider whether analogous side reactions may have significant effects. We have proposed a method of achieving clean Si nanowire growth in a non-UHV ETEM. It is possible that analogous technique may be useful for other growth materials. With this type of protocol, aberration corrected ETEM has exciting prospects for understanding growth mechanisms at the atomic level.

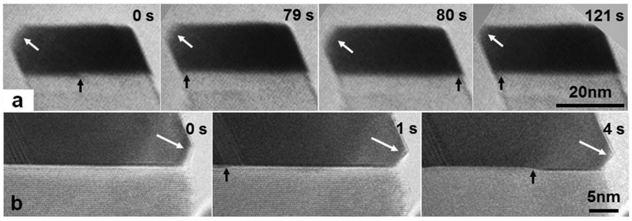

Fig. 4 Rearrangement of the solid catalyst surface. (a) Change in catalyst shape (white arrows) during VSS growth from AuAg at 470 °C and 3×10^{-5} Torr disilane in UHV-TEM. The size of the upper left facet varies during step flow; $1\frac{1}{2}$ cycles are shown. (b) Change in catalyst shape during VSS growth from AuAg in ETEM at 450 °C and 5×10^{-4} Torr disilane.

This work was supported by the National Science Foundation under Grants No. DMR-0606395 and 0907483, the Ministry of Science and Technology R. O. C. under Grant No. NSC-101-2112-M-009-021-MY3 and MOST-104-2112-M-009-015-MY3, the Center for Interdisciplinary Science under the MOE-ATU project for NCTU, ERC Grant 279342: InSituNANO, and the Center for Functional Nanomaterials, Brookhaven National Laboratory, which is supported by the US Department of Energy, Office of Basic Energy Sciences, under contract DE-AC02-98CH10886.

Notes and references

1 F. M. Ross, *Rep. Prog. Phys.*, 2010, **73**, 114501.
2 F. M. Ross, *et al.*, *Phys. Rev. Lett.*, 2005, **95**, 146104.
3 J. B. Hannon, *et al.*, *Nature*, 2006, **440**, 69.
4 S. Kodambaka, *et al.*, *Phys. Rev. Lett.*, 2006, **96**, 96105.
5 P. Madras, *et al.*, *Nano Lett.*, 2009, **9**, 3826.
6 B. A. Wacaser, *et al.*, *Nano Lett.*, 2009, **9**, 3296.
7 S. Kodambaka, *et al.*, *Science*, 2007, **316**, 729.
8 C.-Y. Wen, *et al.*, *Nano Lett.*, 2010, **10**, 514.
9 S. Hofmann, *et al.*, *Nat. Mater.*, 2008, **7**, 372.
10 Y.-C. Chou, *et al.*, *ACS Nano*, 2012, **6**, 6407.
11 C.-Y. Wen, *et al.*, *Science*, 2009, **326**, 1247.
12 C.-Y. Wen, *et al.*, *Phys. Rev. Lett.*, 2011, **107**, 025503.
13 C.-Y. Wen, *et al.*, *Phys. Rev. Lett.*, 2010, **105**, 195502.
14 K. Hiruma, *et al.*, *J. Appl. Phys.*, 1995, **77**, 447; T. I. Kamins, *et al.*, *J. Appl. Phys.*, 2001, **89**, 1008; A. I. Persson, *et al.*, *Nat. Mater.*, 2004, **10**, 677.
15 J. Hu, *et al.*, *Acc. Chem. Res.*, 1999, **32**, 435.
16 C. B. Duke, *Surface Science: The First Thirty Years*, Elsevier, Amsterdam, 1994.
17 A. M. Molenbroek, *et al.*, *Top. Catal.*, 2009, **52**, 1303.
18 H. Yoshida, *et al.*, *Science*, 2012, **335**, 317; Y.-C. Chou, *et al.*, *Microsc. Microanal.*, 2012, **18**(S2), 1084–1085; F. Panciera, *et al.*, *Nat. Mater.*, 2015, **14**, 820.
19 D. Contarato, *et al.*, *Phys. Procedia*, 2013, **37**, 1504.
20 T. Kamino, *et al.*, *Philos. Mag. A*, 1997, **75**, 105.
21 C. Wiethoff, *et al.*, *Nano Lett.*, 2008, **8**, 3065.
22 G. S. Chen, *et al.*, *Philos. Mag. A*, 1998, **78**, 491; N. Jiang, *Rep. Prog. Phys.*, 2016, **79**, 016501.
23 D. J. Stokes, *Principles and practice of variable pressure/environmental scanning electron microscopy*, Wiley, 2008.
24 J. H. Miller, *et al.*, *J. Chem. Phys.*, 1987, **86**, 157.
25 M. Baram, *et al.*, *Science*, 2011, **332**, 206; J. M. Howe, *et al.*, *MRS Bull.*, 2004, **29**, 951; U. Dahmen, *Phys. Rev. Lett.*, 1997, **78**, 471.
26 Y. Yang, *et al.*, *Phys. Rev. Lett.*, 2013, **110**, 096102.
27 J. Tersoff, *et al.*, *Phys. Rev. Lett.*, 1993, **70**, 1143.